Insulin-mTOR hyperfunction drives *C. elegans* aging opposed by the megaprotein LPD-3

Taruna Pandey[1], Bingying Wang[1], Jenny Zu[1], Huichao Deng[2], Kang Shen[2], Goncalo Dias do Vale[3], Jeffrey G. McDonald[3], Dengke K. Ma[1, 4, *]

[1]Cardiovascular Research Institute and Department of Physiology, University of California San Francisco, San Francisco, USA

[2]Department of Biology, Howard Hughes Medical Institute, Stanford University, Stanford, USA

[3]Center for Human Nutrition and Department of Molecular Genetics, University of Texas Southwestern Medical Center, Dallas, USA.

[4]Innovative Genomics Institute, University of California, Berkeley, USA.

* Correspondence: Dengke.Ma@ucsf.edu

Abstract

Decreased insulin-mTOR signaling enables exceptional longevity in the nematode *C. elegans* by activating geroprotective transcription factors, including DAF-16, SKN-1 and HSF-1. Few studies have examined whether and how increased insulin-mTOR may actively drive organismic aging. Here we show that an agonist insulin INS-7 is drastically over-produced and causes shortened lifespan in *lpd-3* mutants, a *C. elegans* model of human Alkuraya-Kučinskas syndrome. Lipidomic profiling reveals marked increase in the abundance of hexaceramide species in *lpd-3* mutants, consistent with up-regulation of the genes encoding biosynthetic enzymes for hexaceramides, including HYL-1 (Homolog of Yeast Longevity). Reducing HYL-1 activity decreases INS-7 levels and rescues the shortened lifespan of *lpd-3* mutants through InsR/DAF-2 and mTOR/LET-363. We propose that increased insulin signaling exhibits late-life antagonistic pleiotropy and shortens lifespans through sphingolipid-hexaceramide and mTOR regulatory pathways.

What causes aging remains a contentious unresolved question. Major theories of aging, including the molecular damage and free radical theory, the antagonistic pleiotropy and hyperfunction theory of aging, have stimulated many studies to test predictions from each[1–6]. A new era in aging research was initiated by the discovery of exceptionally long-lived mutants in *C. elegans*, a genetically tractable model organism particularly suited for aging studies[7–10]. Reduced abundance or activity in components of the insulin pathway (the insulin receptor DAF-2 or PI-3 kinase AGE-1) extends longevity through mechanisms that have been extensively studied and involve activation of geroprotective transcription factors (DAF-16, HSF-1 and SKN-1)[11–13]. While such loss-of-function models have been highly valuable and support critical roles of the insulin/mTOR pathway in aging from diverse organisms, whether and how insulin/mTOR hyperfunction may actively drive aging and age-associated pathological phenotypes still remain largely underexplored.

In recent studies, we identified *lpd-3* in a mutagenesis screen and discovered that the 452 kDa megaprotein LPD-3 is a bridge-like tunnel protein with evolutionarily conserved roles in lipid trafficking from endoplasmic reticulum to plasma membranes (Fig. 1a)[14]. Mutations in *BLTP1*, the human orthologue of *lpd-3*, cause an autosomal recessive Alkuraya-Kucinskas syndrome (AKS)[15–17]. Since most AKS patients die prematurely, we sought to determine the lifespan of *lpd-3* mutants in *C. elegans*. We generated two backcrossed strains carrying a deletion allele *ok2138* or CRISPR-generated stop-codon allele *wy1772*, respectively (Fig. 1b). Both strains showed strikingly shortened lifespans at three temperature culture conditions tested (Fig. 1c-e). As *lpd-3* is expressed as multiple isoforms (Wormbase) and we were unable to generate viable strains with whole-gene deletions, neither allele tested for lifespan likely produces null functions. In addition to shorten overall lifespan, we found *lpd-3* mutants exhibit various aging phenotypes, including pharyngeal pumping and locomotion that decline earlier than in wild type (Supplementary Fig. 1).

The drastically shortened lifespan of *lpd-3* mutants prompted us to seek to identify the underlying mechanisms. By analyzing RNA-seq datasets for *lpd-3* mutants compared to wild type[14], we discovered that LPD-3 deficiency led to nearly 40-fold increase in the expression level of *ins-7*, which represents one of the most highly *lpd-3* up-regulated genes and encodes an agonist insulin with previously reported effects on aging and lifespan in *C. elegans*[18–20] (Fig. 1f). Expression of other insulin-encoding genes was much less regulated or largely unaltered (Supplementary Fig. 2a, b). To determine the spatiotemporal site of *ins-7* regulation, we crossed an integrated *ins-7*p::*ins-7*::GFP translational reporter strain[21] with *lpd-3* deletion mutants. In the wild type, *ins-7*p::*ins-7*::GFP is expressed at baseline levels that are detectable only in the anterior intestine at 15 ^{o}C starting from young adult stages, and increased at 20 ^{o}C and 25 ^{o}C (Fig. 1g). By contrast, *ins-7*p:: *ins-7*::GFP in *lpd-3* mutants showed drastically increased GFP abundance throughout the intestine, and particularly at higher cultivation temperatures (25 ^{o}C). We showed previously that *lpd-3* mutants are defective in ER-to-PM phospholipid trafficking, exhibit sensitivity to thermal stress that can be normalized by Lecithin[14]. We confirmed in this study that both shortened lifespan and *ins-7* up-regulation phenotypes were also rescued by Lecithin (Supplementary Fig. 2c, d).

To determine the causal role of *ins-7* in the shortened lifespan phenotype of *lpd-3* mutants, we used RNAi to knockdown *ins-7* expression in *lpd-3* mutants. We found treatment with RNAi against *ins-7* led to markedly extended lifespan of *lpd-3* mutants, comparable to that in the wild type (Fig. 1h). We also observed such rescue of shortened lifespan phenotype of *lpd-3* mutants by RNAi against *daf-2* (Fig. 1i), which encodes the only known receptor of insulin in *C. elegans*. We note that control RNAi also led to a slight increase of lifespan in *lpd-3* mutants (Fig. 1d, h), likely reflecting different lipid compositions of bacterial strains between OP50 and HT115 strains[22,23] used in routine *C. elegans* culture and RNAi experiments, respectively. Reducing *ins-7* expression

has been previously shown to increase lifespan of wild-type animals, implicating INS-7's role in tissue entrainment by feedback regulation in *C. elegans*[18–20]. Our results support these early findings and reveal that overproduction of INS-7 is causally responsible for shortening lifespan in *lpd-3* mutants, in a manner that requires the sole insulin receptor DAF-2 (Fig. 1j).

We next determined the regulatory mechanisms leading to *ins-7* up-regulation and shortened lifespan in *lpd-3* mutants. Taking advantage of the drastically up-regulated *ins-7*p::*ins-7*::GFP reporter in *lpd-3* mutants as a live fluorescent readout, we performed targeted RNAi screens to identify genes required for *ins-7*p::*ins-7*::GFP up-regulation by *lpd-3*. We performed RNAi for those genes with reported adequate expression in the intestine (transcript per million, TPM > 2) and encoding mediators of major signal transduction pathways known to be involved in insulin signaling (the Ras/MAPK, phospholipase C and PI3 kinase/mTORC1/mTORC2 pathways)[24–26] (Supplementary Fig. 3). As positive controls, we verified strong effects of *ins-7* or *daf-2* RNAi in suppressing *ins-7*p::*ins-7*::GFP expression in *lpd-3* mutants (Fig. 2a, b). From such screens, we found that RNAi against several genes encoding components of the mTORC2 complex in *C. elegans*, including *let-363*, *rict-1* and *sinh-1*, led to marked reduction of *ins-7*p::*ins-7*::GFP in *lpd-3* mutants (Fig. 2a, b). RNAi against genes involved in the mTORC1 complex, except *let-363* shared by mTORC1 and mTORC2, exhibited weaker effects (Fig. 2a).

In parallel to such RNAi screens, we also performed lipidomic profiling of *lpd-3* mutants compared to wild type. Among all major lipid species examined by LC-MS/MS, including phospholipids, glycerolipids and sphingolipids (Supplementary Table 1), the hexaceramide-type of sphingolipids showed marked up-regulation in *lpd-3* mutants (Fig. 2c). Consistently, RNA-seq results revealed that genes encoding hexaceramide biosynthetic enzymes (Fig. 2d), including HYL-1 and CGT-1/2/3, were markedly up-regulated in *lpd-3* mutants (Fig. 2e). As reduced LPD-3 activity results

in impaired ER-to-PM phospholipid trafficking, a compensatory lipid homeostatic mechanism is likely triggered to up-regulate sphingolipids in *lpd-3* mutants[14]. Given reported sphingolipid modulation of mTOR signaling and longevity[27–29], we next explored specifically the link of hexaceramide biosynthetic enzyme HYL-1 to *ins-7* and found that *hyl-1* RNAi led to strong suppression of *ins-7*p::*ins-7*::GFP in *lpd-3* mutants. Functionally, lifespan analysis revealed that RNAi against *rict-1* or *hyl-1* led to marked rescue of the shortened lifespan in *lpd-3* mutants (Fig. 2f, g). RNAi against *sgk-1*, which encodes a major kinase mediating effects of mTORC2, showed similar rescuing effects (Fig. 2h). Taken together, these results indicate that the sphingolipid-mTOR pathway drives *ins-7* over-expression, leading to the shortened lifespan in *lpd-3* mutants.

Identification and subsequent mechanistic studies of exceptionally long-live *C. elegans* mutants in the insulin/mTOR pathway have provided crucial insights into how loss of insulin/mTOR function extends longevity. Activation of key transcription factors including DAF-16, HSF-1 and SKN-1 mediates geroprotective effects in these mutants by promoting somatic maintenance programs that attenuate molecular and cellular damages. Our studies provide a novel and complementary model in which we propose insulin/mTOR hyperfunction can actively drive aging downstream of the sphingolipid-ceramide pathway (Supplementary Fig. 4). Various sphingolipids have been shown to contribute to organismic aging and age-associated pathologies[30–32]. We identify LPD-3 as a critical megaprotein regulator of the phospholipid-sphingolipid rheostat, dysfunction of which can profoundly affect aging via insulin/mTOR. Detailed mechanisms linking LPD-3 to sphingolipid regulation, insulin over-production and aging await further studies. Based on our findings and prior evidence supporting early-life beneficial and late-life detrimental roles of sphingolipid/ceramides and insulin-mTOR signaling, we propose that the sphingolipid-insulin-mTOR axis may exhibit antagonistic pleiotropy in driving aging of phylogenetically diverse organisms.

Methods

C. elegans culture and maintenance

All the *C. elegans* strains used in the current research were maintained in accordance with the standard laboratory procedures unless otherwise stated. Genotypes of strains used are as follows: N2 Bristol strain (wild type), Chr. I: *lpd-3*(*ok2138*), *lpd-3*(*wy1772*); Chr. III: *yxIs13* III [*ins-7*p::*gfp*; *unc-122*p::*dsred*].

Lifespan assessment

The lifespan assay was conducted according to the standard protocol. Briefly, wild type N2 strain was grown for 2 generations without starvation, then embryos were extracted through standard Sodium hypochlorite treatment. These embryos were transferred to RNAi seeded NGM plates. Thereafter, 50-100 late L4 larvae or young adults were transferred to RNAi seeded NGM plates supplemented with 50 μM of 5-fluoro-2-deoxyuridine (FUDR, Sigma) to prevent progeny growth and were shifted to fresh plate every 3-4 days[33]. Live/dead/missing worms were scored on alternate days till last surviving worm. The live worms were detected through touch provoke responses. The lifespan assays were repeated for at least three independent trials.

Epifluorescence microscopic imaging

The epifluorescence compound microscope (Leica ctr5000) was used to capture fluorescence images. The young adult worms of various genotypes/ treated with different RNAi were randomly

picked and treated with 10 mM sodium azide in M9 solution (Sigma-Aldrich), symmetrically aligned on 2% agar pads on slides for imaging[34]. The control and treatment groups were imaged under identical setting and conditions.

Behavioral studies

The locomotion of worms was measured as previously described[35]. Briefly, the speed (total track length/time) of age-synchronized worms were recorded using WormLab System (MBF Bioscience) based on midpoint position of the worms at different time points. The experiment was repeated thrice with more than 10 animals per group. For pharyngeal pumping assay[36], counting a cycle of synchronous contraction and relaxation of the corpus and the terminal bulb was scored using stereomicroscope (UNITRON Z850) at 50X magnification for each strain, at least 10 worms were scored for each trial.

Lipidomic analysis

Wild type N2 strain and *lpd-3*(*ok2138*) mutants were grown under non-starved conditions for four generations at 20 ºC, followed by bleach synchronization and harvest by M9 buffer at young adult stages. Frozen worm pellets (50 µl per sample, three independent biological replicates per genotype) are stored until lipidomic extraction and analysis. All solvents for lipidomic extraction and analysis used were either HPLC or LC/MS grade and purchased from Sigma-Aldrich (St Louis, MO, USA). Splash Lipidomix standards were purchased from Avanti (Alabaster, AL, USA). All lipid extractions were performed in 16×100mm glass tubes with PTFE-lined caps (Fisher Scientific, Pittsburg, PA, USA). Glass Pasteur pipettes and solvent-resistant plasticware pipette tips (Mettler-Toledo, Columbus, OH, USA) were used to minimize leaching of polymers

and plasticizers. Samples were transferred to fresh glass tubes, and 1 mL of methanol, 1mL of water and 2mL of methyl tert-butyl ether (mTBE) was added for for liquid-liquid extraction. The mixture was vortexed and centrifuged at 2,671 g for 5 min, resulting in two distinct liquid phases. The organic phase (upper phase) was transferred to a fresh tube with a Pasteur pipette and spiked with 20uL of a 1:5 diluted Splash Lipidomix standard mixture. The samples were dried under N_2 and resuspended in 400 µL of hexane. Lipids were analyzed by LC-MS/MS using a SCIEX QTRAP 6500^+ (SCIEX, Framingham, MA) equipped with a Shimadzu LC-30AD (Shimadzu, Columbia, MD) high-performance liquid chromatography (HPLC) system and a 150×2.1 mm, 5 µm Supelco Ascentis silica column (Supelco, Bellefonte, PA). Samples were injected at a flow rate of 0.3 ml/min at 2.5% solvent B (methyl tert-butyl ether) and 97.5% Solvent A (hexane). Solvent B was increased to 5% over 3 min and then to 60% over 6 min. Solvent B was decreased to 0% during 30 sec while Solvent C (90:10 (v/v) isopropanol-water) was set at 20% and increased to 40% during the following 11 min. Solvent C is increased to 44% over 6 min and then to 60% over 50 sec. The system was held at 60% solvent C for 1 min prior to re-equilibration at 2.5% of solvent B for 5 min at a 1.2 mL/min flow rate. Solvent D [95:5 (v/v) acetonitrile-water with 10 mM Ammonium acetate] was infused post-column at 0.03 ml/min. Column oven temperature was 25°C. Data was acquired in positive and negative ionization mode using multiple reaction monitoring (MRM). The LC-MS/MS data was analyzed using MultiQuant software (SCIEX). The identified lipid species were normalized to its corresponding internal standard.

Statistics and reproducibility

All the data in the current manuscript were analyzed using GraphPad Prism 9.2.0 Software (Graphpad, San Diego, CA) and presented as means ± S.D. unless otherwise specified, with

significance *P* values calculated by unpaired two-sided *t*-tests (comparisons between two groups), one-way or two-way ANOVA (comparisons across more than two groups) and adjusted with Bonferroni's corrections. Lifespan assay was quantified using Kaplan–Meier lifespan analysis and *P* values were calculated using log-rank test.

Acknowledgments

Some strains were provided by Dr. Yun Zhang and *Caenorhabditis* Genetics Center (CGC), which is funded by NIH Office of Research Infrastructure Programs (P40 OD010440). The work was supported by NIH grant 1R35GM139618, UCSF PBBR New Frontier Research (D.K.M).

Author contributions

T.P., B.W., J.Z. and D.K.M. designed, performed and analyzed most of the *C. elegans* experiments, contributed to project conceptualization and wrote the manuscript. G.V. and J.G.M. contributed to lipid analysis. H.D. and K.S. contributed to the CRISPR allele generation and project conceptualization. D.K.M. supervised the project.

Competing interests

The authors declare no competing interests.

Materials & Correspondence.

Correspondence and material requests should be addressed to Dengke K. Ma, Ph.D. (dengke.ma@ucsf.edu).

Figures and Figure legends

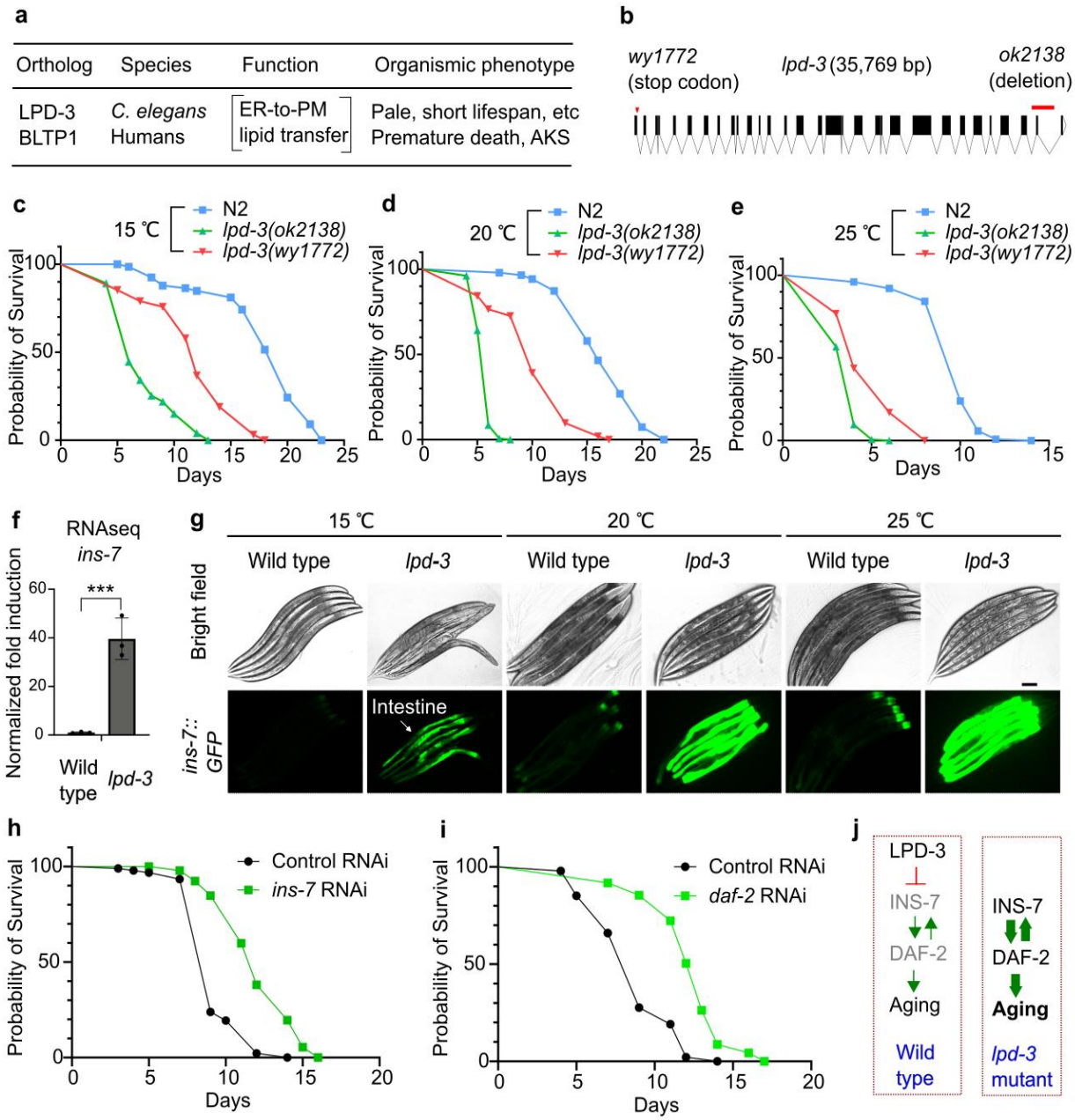

Fig. 1 Hyper-activation of *ins-7* causes shortened lifespan in *lpd-3* mutants. a, Cellular function and organismic phenotypes for LPD-3 and the human homologue BLTP1. **b**, Gene diagram showing two alleles of *lpd-3* examined for lifespan phenotypes. **c**, Lifespan analysis of wild type versus *lpd-3* mutants with two different alleles (*ok2138* and *wy1772*) grown at 15 ^{o}C. **d**,

Lifespan analysis of wild type versus *lpd-3* mutants with two different alleles (*ok2138* and *wy1772*) grown at 20 ^{o}C. **e**, Lifespan analysis of wild type versus *lpd-3* mutants with two different alleles (*ok2138* and *wy1772*) grown at 25 ^{o}C. **f**, RNA-seq results showing increased *ins-7* expression in *lpd-3* mutants. Values are means ± S.D. *** indicates $P < 0.001$ (N = 3 biological replicates). **g**, Representative bright field and epifluorescence images showing increased *ins-7*p::*ins-7*::GFP abundance in *lpd-3* mutants. Scale bar, 100 µm. **h**, Lifespan analysis of *lpd-3* mutants with control or *ins-7* RNAi at 20 ^{o}C, showing shortened lifespan rescued ($P < 0.0001$, log-rank test). **i**, Lifespan analysis of *lpd-3* mutants with control or *daf-2* RNAi at 20 ^{o}C, showing shortened lifespan rescued ($P < 0.0001$, log-rank test). **j**, Schematic diagrams illustrating a model of how LPD-3 regulates aging via INS-7 and DAF-2 in wild type and *lpd-3* mutants.

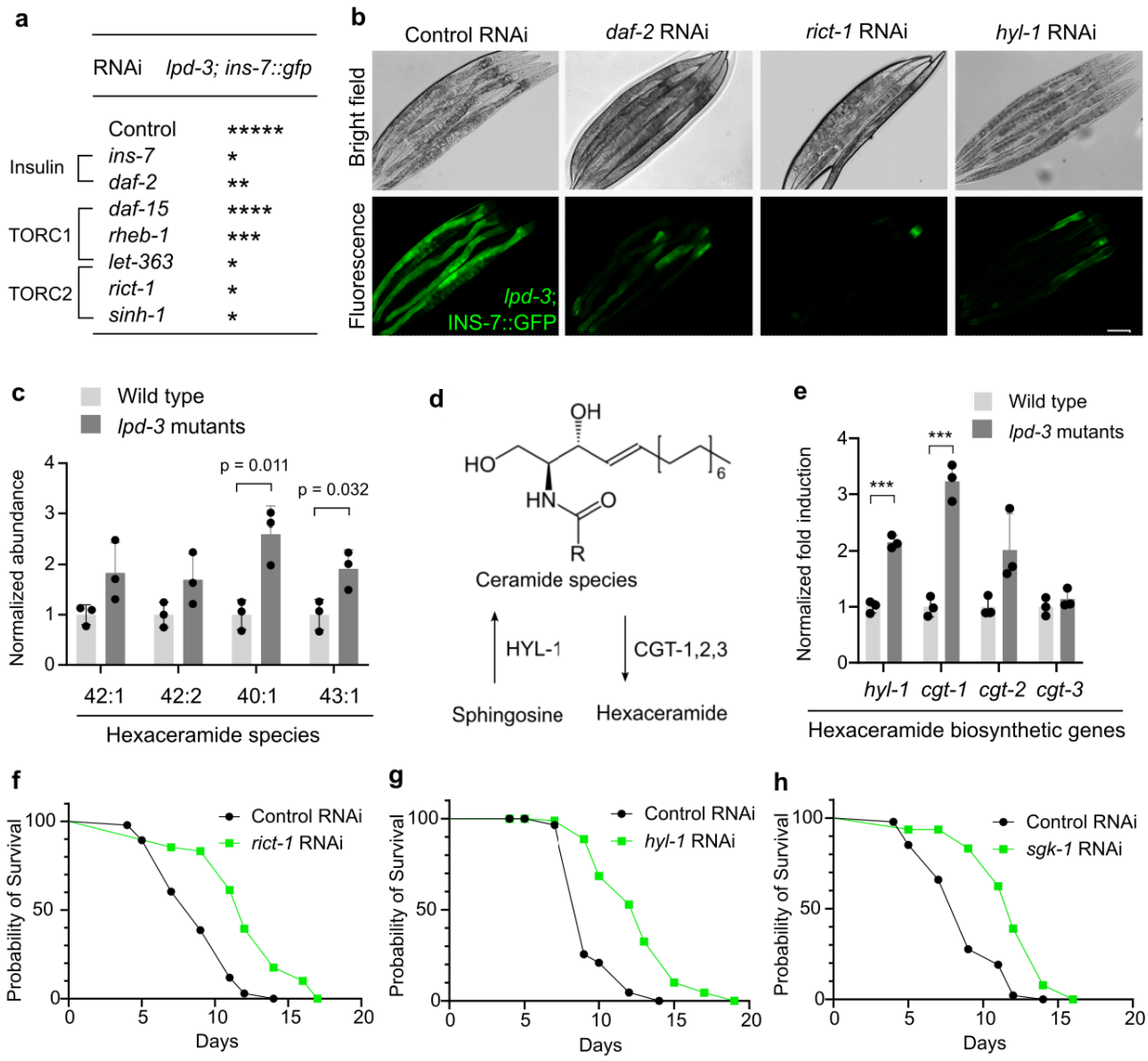

Figure 2. The sphingolipid-ceramide, INS-7/insulin and mTOR axis drives aging in *lpd-3* mutants. a, Table summarizing effects of RNAi against genes in the insulin/mTORC1/mTORC2 pathway on *ins-7*p::*ins-7*::GFP levels in *lpd-3* mutants. **b**, Representative bright field and epifluorescence images showing *ins-7*p::*ins-7*::GFP up-regulation in *lpd-3* mutants can be suppressed by RNAi against *daf-2*, *rict-1* or *hyl-1*. Scale bar, 100 µm. **c**, Lipidomic quantification of hexaceramide species in wild type and *lpd-3* mutants. Values are means ± S.D. (N = 3 biological replicates). **d**, Schematic showing biosynthetic pathways of hexaceramide, including sphingosine

conversion to ceramide by HYL-1 and ceramide to hexaceramide by CGT-1/2/3. **e**, RNA-seq results showing increased *hyl-1* and *cgt-1/2/3* expression in *lpd-3* mutants. Values are means ± S.D. ***$P < 0.001$ (N = 3 biological replicates). **f**, Lifespan analysis of *lpd-3* mutants with control or *rict-1* RNAi at 20 ^{o}C, showing rescued lifespan ($P < 0.0001$, log-rank test). **g**, Lifespan analysis of *lpd-3* mutants with control or *hyl-1* RNAi at 20 ^{o}C, showing rescued lifespan ($P < 0.0001$, log-rank test). **h**, Lifespan analysis of *lpd-3* mutants with control or *sgk-1* RNAi at 20 ^{o}C, showing rescued lifespan ($P < 0.0001$, log-rank test).

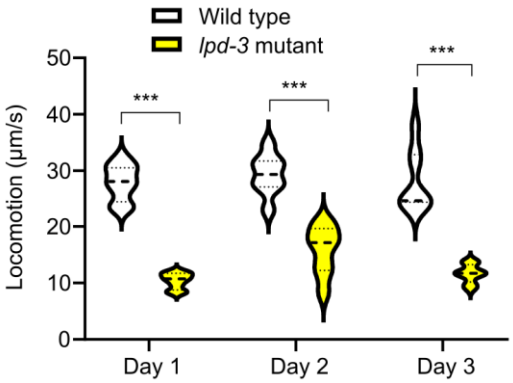

Supplementary Figure 1. Behavioral declines of *lpd-3* mutants early in aging. Quantification of locomotion for wild type and *lpd-3* mutants showing more rapid decline in *lpd-3* mutants starting at day 1 (24 hrs post-L4 stage). *** indicates $P < 0.001$ (N = 30-50 animals per group).

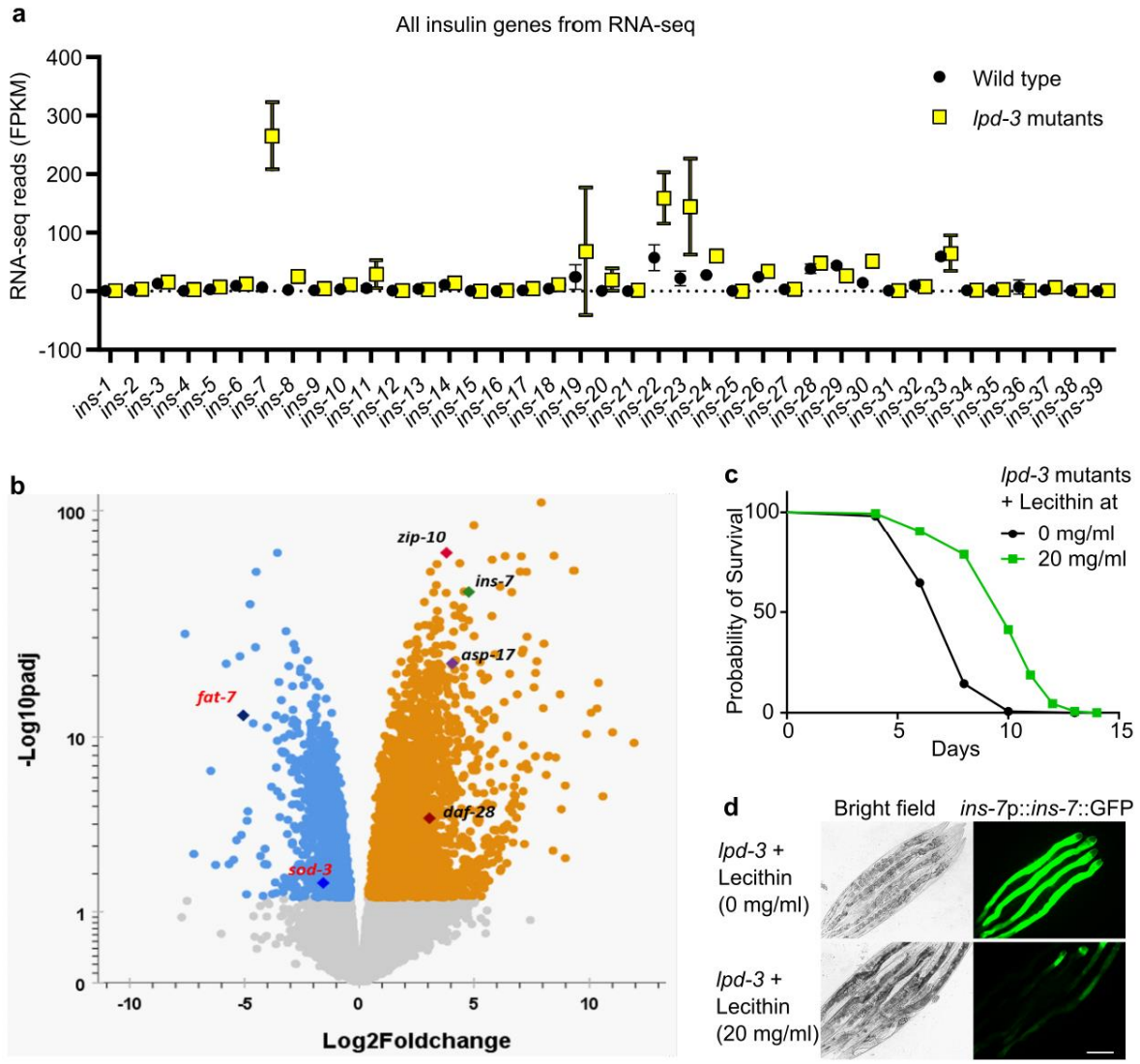

Supplementary Fig. 2 Specific up-regulation of *ins-7* by loss of LPD-3 and rescue by Lecithin.

a, RNA-seq reveals drastic and specific *ins-7* up-regulation among all *ins* genes examined. Results were derived and analyzed from RNA-seq datasets we published earlier[14]. FPKM, Fragments Per Kilobase of transcript per Million mapped reads. **b**, Volcano plot showing significantly LPD-3 regulated genes, including *fat-7* (downstream of SBP-1 and NHR-49), *sod-3* (downstream of DAF-16) and *zip-10* (downstream of ISY-1), *asp-17* (downstream of ISY-1), and *ins-7*. **c**, Lifespan analysis of *lpd-3* mutants with control or Lecithin treatment at 20 ºC ($P < 0.0001$, log-rank test).

d, Representative bright field and epifluorescence images showing that *ins-7*p::*ins-7*::GFP up-regulation in *lpd-3* mutants can be suppressed by exogenous Lecithin (20 mg/ml) treatment in culture media. Scale bar, 100 µm.

Signal transduction pathways	**Genes tested for RNAi effects in *lpd-3; ins-7*::GFP**
(Cytoplasmic signaling proteins and transcription factors)	(Selected with intestinal TPM expression > 2.0) (Red: GFP abundance decreased)
Insulin	*ins-7*, *daf-28*
Insulin receptors	*daf-2*
PI3 kinases	*age-1*
mTORC1 kinase complex	*daf-15, mlst-8, raga-1, rheb-1, let-363*
mTORC2 kinase complex	*rict-1, let-363, sgk-1, sinh-1*
MAP kinases	*pmk-1, pmk-3, jnk-1, kgb-1, kgb-2, jkk-1, mek-1*
Phospholipases	*plc-1, plc-2, plc-4*
Transcription factors	*daf-16, hsf-1, skn-1, hif-1, hlh-30, atfs-1, yap-1, sta-2*

Supplementary Fig. 3 RNAi screens for genes affecting *ins-7* in *lpd-3* mutants.

Genes were selected for RNAi testing given their adequate expression values in intestine (TPM or transcript per million > 2.0) and putative roles in mediating insulin/mTOR signaling.

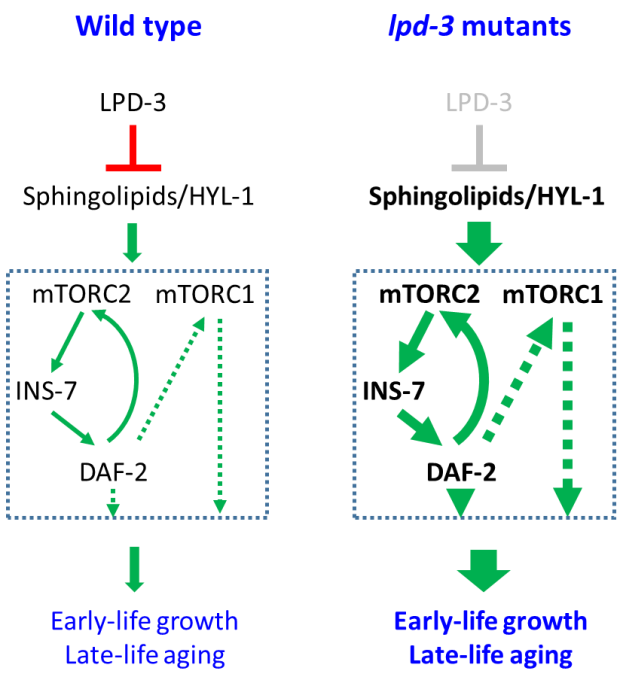

Supplementary Fig. 4 Model.

In the wild type, LPD-3 mediates phospholipid trafficking from ER to PM, and in turn, suppresses sphingolipid levels. Insulin and mTOR signaling are activated at moderate levels to promote early-life growth and late-life aging. In the *lpd-3* mutants, reduced LPD-3 function leads to sphingolipid (hexaceramide type) up-regulation and hyperactivation of insulin and mTOR signaling. INS-7/DAF-2/mTORC2 forms a proposed vicious cycle to sustain insulin and mTOR activation through a positive feedback loop, culminating in hastened late-life aging and shortened lifespan. Red indicates inhibition, while green indicates activation. Solid arrows indicate proposed action based on this study, while dashed arrows indicate regulation based on evidence from literature.

Supplementary Table 1 Lipidomic profiling of phospholipids, glycerolipids and sphingolipids.

References

1. Gems, D. The hyperfunction theory: An emerging paradigm for the biology of aging. *Ageing Res Rev* **74**, 101557 (2022).
2. Gladyshev, V. N. Aging: progressive decline in fitness due to the rising deleteriome adjusted by genetic, environmental, and stochastic processes. *Aging Cell* **15**, 594–602 (2016).
3. Longo, V. D., Mitteldorf, J. & Skulachev, V. P. Programmed and altruistic ageing. *Nat Rev Genet* **6**, 866–872 (2005).
4. de Magalhães, J. P. & Church, G. M. Genomes optimize reproduction: aging as a consequence of the developmental program. *Physiology (Bethesda)* **20**, 252–259 (2005).
5. Gladyshev, V. N. The Free Radical Theory of Aging Is Dead. Long Live the Damage Theory! *Antioxid Redox Signal* **20**, 727–731 (2014).
6. Sohal, R. S. & Weindruch, R. Oxidative stress, caloric restriction, and aging. *Science* **273**, 59–63 (1996).
7. Kenyon, C. J. The genetics of ageing. *Nature* **464**, 504–512 (2010).
8. Klass, M. R. A method for the isolation of longevity mutants in the nematode Caenorhabditis elegans and initial results. *Mech Ageing Dev* **22**, 279–286 (1983).
9. Kenyon, C., Chang, J., Gensch, E., Rudner, A. & Tabtiang, R. A C. elegans mutant that lives twice as long as wild type. *Nature* **366**, 461–464 (1993).
10. Finch, C. E. & Ruvkun, G. The genetics of aging. *Annu Rev Genomics Hum Genet* **2**, 435–462 (2001).
11. Tullet, J. M. A. *et al.* Direct inhibition of the longevity-promoting factor SKN-1 by insulin-like signaling in C. elegans. *Cell* **132**, 1025–1038 (2008).

12. Ogg, S. *et al.* The Fork head transcription factor DAF-16 transduces insulin-like metabolic and longevity signals in C. elegans. *Nature* **389**, 994–999 (1997).

13. Hsu, A.-L., Murphy, C. T. & Kenyon, C. Regulation of aging and age-related disease by DAF-16 and heat-shock factor. *Science* **300**, 1142–1145 (2003).

14. Wang, C. *et al.* A conserved megaprotein-based molecular bridge critical for lipid trafficking and cold resilience. *Nat Commun* **13**, 6805 (2022).

15. Kane, M. S. *et al.* Endosomal trafficking defects in patient cells with KIAA1109 biallelic variants. *Genes Dis* **6**, 56–67 (2019).

16. Gueneau, L. *et al.* KIAA1109 Variants Are Associated with a Severe Disorder of Brain Development and Arthrogryposis. *Am J Hum Genet* **102**, 116–132 (2018).

17. Meszarosova, A. U. *et al.* Two novel pathogenic variants in KIAA1109 causing Alkuraya-Kučinskas syndrome in two Czech Roma brothers. *Clin Dysmorphol* **29**, 197–201 (2020).

18. Murphy, C. T., Lee, S.-J. & Kenyon, C. Tissue entrainment by feedback regulation of insulin gene expression in the endoderm of Caenorhabditis elegans. *Proc Natl Acad Sci U S A* **104**, 19046–19050 (2007).

19. Murphy, C. T. *et al.* Genes that act downstream of DAF-16 to influence the lifespan of Caenorhabditis elegans. *Nature* **424**, 277–283 (2003).

20. Lee, Y. *et al.* Reduced insulin/IGF1 signaling prevents immune aging via ZIP-10/bZIP-mediated feedforward loop. *J Cell Biol* **220**, e202006174 (2021).

21. Chen, Z. *et al.* Two insulin-like peptides antagonistically regulate aversive olfactory learning in C. elegans. *Neuron* **77**, 572–585 (2013).

22. Neve, I. A. A. *et al.* Escherichia coli Metabolite Profiling Leads to the Development of an RNA Interference Strain for Caenorhabditis elegans. *G3 (Bethesda)* **10**, 189–198 (2019).

23. Brooks, K. K., Liang, B. & Watts, J. L. The Influence of Bacterial Diet on Fat Storage in C. elegans. *PLoS One* **4**, e7545 (2009).

24. Taylor, S. R. *et al.* Molecular topography of an entire nervous system. *Cell* **184**, 4329-4347.e23 (2021).

25. Saltiel, A. R. Insulin signaling in health and disease. *J Clin Invest* **131**, e142241, 142241 (2021).

26. Blackwell, T. K., Sewell, A. K., Wu, Z. & Han, M. TOR Signaling in Caenorhabditis elegans Development, Metabolism, and Aging. *Genetics* **213**, 329–360 (2019).

27. Thorner, J. TOR complex 2 is a master regulator of plasma membrane homeostasis. *Biochem J* **479**, 1917–1940 (2022).

28. Zhu, H., Shen, H., Sewell, A. K., Kniazeva, M. & Han, M. A novel sphingolipid-TORC1 pathway critically promotes postembryonic development in Caenorhabditis elegans. *Elife* **2**, e00429 (2013).

29. Taniguchi, M. *et al.* Regulation of autophagy and its associated cell death by ‘sphingolipid rheostat’: reciprocal role of ceramide and sphingosine 1-phosphate in the mammalian target of rapamycin pathway. *J Biol Chem* **287**, 39898–39910 (2012).

30. Tang, H., Huang, X. & Pang, S. Regulation of the lysosome by sphingolipids: Potential role in aging. *J Biol Chem* **298**, 102118 (2022).

31. Trayssac, M., Hannun, Y. A. & Obeid, L. M. Role of sphingolipids in senescence: implication in aging and age-related diseases. *J Clin Invest* **128**, 2702–2712.

32. Laurila, P.-P. *et al.* Sphingolipids accumulate in aged muscle, and their reduction counteracts sarcopenia. *Nat Aging* **2**, 1159–1175 (2022).

33. Sutphin, G. L. & Kaeberlein, M. Measuring Caenorhabditis elegans life span on solid media. *J Vis Exp* 1152 (2009) doi:10.3791/1152.

34. Bargmann, C. I. & Avery, L. Laser killing of cells in Caenorhabditis elegans. *Methods Cell Biol* **48**, 225–250 (1995).

35. Vozdek, R., Long, Y. & Ma, D. K. The receptor tyrosine kinase HIR-1 coordinates HIF-independent responses to hypoxia and extracellular matrix injury. *Sci Signal* **11**, (2018).

36. Hobson, R. J. *et al.* SER-7, a Caenorhabditis elegans 5-HT7-like receptor, is essential for the 5-HT stimulation of pharyngeal pumping and egg laying. *Genetics* **172**, 159–169 (2006).